LATTICE STUDIES FOR CIRCE (Coherent InfraRed CEnter) AT THE ALS*

Hiroshi Nishimura, David Robin, Fernando Sannibale and Weishi Wan
LBNL, Berkeley, CA 94720, USA

Abstract

CIRCE (Coherent InfraRed CEnter) at the Advanced Light Source, Lawrence Berkeley National Lab (LBNL), is a proposal for a new electron storage ring optimized for the generation of coherent synchrotron radiation (CSR) in the terahertz frequency range. One of the main requirement for this special mode of operation is the capability of the ring of operating at small momentum compaction values. In this regime, the longitudinal dynamics becomes strongly nonlinear and an accurate control of the higher order energy dependent terms of the momentum compaction is necessary. The lattice for CIRCE allows controlling these terms up to the third order. The paper describes the lattice and presents the calculated performances in terms of momentum acceptance, dynamic aperture, lifetime and momentum compaction tune capabilities.

INTRODUCTION

A general description of CIRCE, including its background and applications, is given in the companion paper[1]. Here, we analyze the case for the parameters of CIRCE given in Table 1. It is worth to remark that we assume an RF voltage of 0.6 MV (notmal conducting RF system), while in reference[1] we upgraded the RF system to superconductive with 1.2 MV RF voltage. The analysis of this new configuration is under way.

Table 1: Basic Parameters

Parameter	Value
Circumference (m)	66
Symmetry	6
Beam energy (MeV)	600
Bending radius (m)	1.335
Betatron tune ν_x	5.15
ν_y	4.20
RF frequency (GHz)	1.5
voltage (MV)	0.6
Harmonic number	330
Radiation loss/turn (KV)	8.6

Three sets for different modes of operation are considered and listed in Table 2. In what follows, we focus our attention on Set 3 because with its higher current density is the more critical in terms of beam lifetime.

* Work supported by the U.S. Department of Energy under Contract No. DE-AC03-76SF00098

Table 2: Small-α Operation

	Set 1	Set 2	Set 3
Pulse length, rms, (ps)	1.0	2.0	3.0
Total current (mA)	8.0	35	90
Current per bunch (μA)	24.0	106	272
Particles per bunch(10^7)	3.3	15	37
Mom.compaction(10^{-4})	2.4	8.6	19

UNIT CELL

The CIRCE storage ring uses a unit cell 11-m long with a double-bend arc. The symmetry is 6 therefore each bend gives 30° of bending. There are 3 pairs of quadrupoles (Q1 $\sim$ Q3) and sextupoles (S1 $\sim$ S3) per unit cells as the one shown in Fig. 1. Octupoles (O1 $\sim$ O3) are also available as embedded components in quadrupoles. The beta functions and dispersion of Set 3 are shown in Fig. 2. Their values at the beginning of the cell are $\beta_x = 3.84$ m, $\beta_y = 2.93$ m and $\eta_x = -0.17$ m.

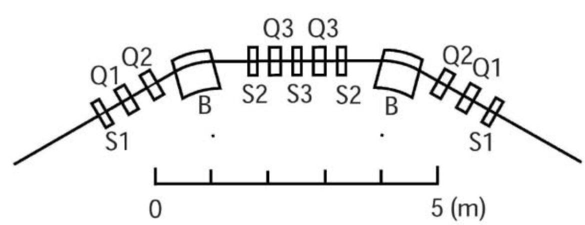

Figure 1: Unit cell

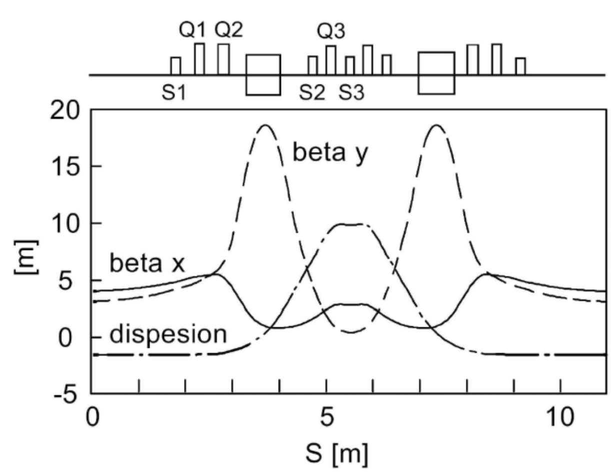

Figure 2: Beta and Dispersion

BENDING MAGNET

The 30° bending magnet of CIRCE has the peculiar shape of a parallel face dipole with defocusing gradient and with lamination shifted to follow the beam trajectory (see Type C in Fig.3). We found that such a geometry cannot be modeled by the standard 4x5 formalism that uses the linearized Hamiltonian in the curved coordinate (Type A in Fig.3) with artificial thin quadrupole elements on both sides of it. It must be treated as that of compact storage rings without using a large-ring approximation to linearize the Hamiltonian. A symplectic integrator must be used for both the lattice design and the article tracking studies with accurate off-energy properties for fine tuning of the momentum compaction factor (α). The linear expansion of a kinetic term of the Hamiltonian should be avoided and the effect of wedges and the fringe fields have to be treated properly. We found that the use of the type B geometry in Fig.3 with the Bingo[2] integrator in cartesian coordinate is preferable.

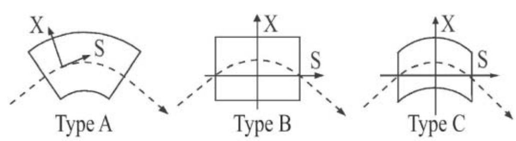

Figure 3: Geometry of a bending magnet

The remaining issue is the effect of the mechanical curvature of the laminated plates that are shifted along the reference orbit with a constant bending radius. We modified the symplectic Bingo integrator implemented in the C++ code Goemon[3] by introducing a longitudinal (s) dependence in the potential of the Hamiltonian:

$$\begin{aligned} H = & -((1+\delta)^2 - p_x^2 - p_y^2)^{\frac{1}{2}} + \delta \\ & + \tfrac{k}{2}((x - x_0(s))^2 - y^2) \end{aligned} \qquad (1)$$

where x, y, p_x and p_y are horizontal and vertical coordinates and momentum, $\delta = (p - p_0)/p_0$ with p and p_0 the total momentum and the nominal momentum respectively, and $x_0(s)$ is the horizontal coordinate of the reference orbit.

Table 3 shows the effect of the different geometries on the natural chromaticity (ζ_x and ζ_y) and the natural emittance (ε_0) for Lattice A in Table 5. The values are calculated by using Goemon. MAD 8 is also used for comparison purpose.

Table 3: Comparison of Chromaticity and Emittance

Type[1]	Code	ζ_x	ζ_y	ε_0
A	Goemon(4x5)	-5.13	-16.28	3.2×10^{-8}
B	Goemon(Bingo)	-5.22	-24.26	3.2×10^{-8}
C	Goemon(Bingo)	-5.20	-24.48	3.2×10^{-8}
	MAD 8[2]	-5.19	-24.78	3.0×10^{-8}

[1]Types in Fig. 3. [2]SBEND is used.

Table 3 indicates that the effect of the mechanical curvature is not relevant as far as the chromaticity and the emittance concern. However, there are non-negligible differences in the quadrupole settings and the horizontal beta function (β_x) as listed in Table 4. Therefore, we decided to use the modified Bingo integrator for the computations on CIRCE.

Table 4: Comparison of Chromaticity and Emittance

Type	Q1	Q2	Q3	β_x^*	β_y^*
B	0.810	4.138	3.607	3.43	2.98
C	0.635	4.375	3.607	3.15	3.14

*At the center of the straight section (m)

FITTING OF MOMENTUM-COMPACTION

Momentum Compaction As the momentum compaction becomes smaller, its higher order components become relevant. We expand it to the 4-th order as in Eq.(2) and will fit the first three terms.

$$\frac{\delta C}{C_0} = \alpha_1(\frac{\delta p}{p_0}) + \alpha_2(\frac{\delta p}{p_0})^2 + \alpha_3(\frac{\delta p}{p_0})^3 + \alpha_4(\frac{\delta p}{p_0})^4 \qquad (2)$$

where C_0 is a nominal path length, δC is the path-lengthening due to a momentum deviation of δp.

Table 5: Parameter Fitting

Lattice	A	B	C	D
Quadrupole Q1 (m^{-1})	0.810		0.650	
Q2 (m^{-1})	4.138		4.230	
Q3 (m^{-1})	3.607		3.751	
Sextupole S1 (m^{-2})	0	0	0	7.16
S2 (m^{-2})	0	-35.6	-30.8	-32.5
S3 (m^{-2})	0	46.3	-40.9	-37.8
Octupole O3 (m^{-3})	0	0	0	-46.6
Dispersion$^*\eta_x(m)$	0	0	-0.17	-0.17
Chromaticity ζ_x	-5.20	0	0	0
ζ_y	-24.5	0	0	0
Mom. compaction α_1	6.0×10^{-3}		1.9×10^{-3}	
α_2	0.11	-0.04	-0.05	0
α_3	-1.16	-1.79	-1.90	0
α_4	13.2	-22.9	-17.8	1.09
Emittance ε_0 (m·rad)	3.2×10^{-8}		5.6×10^{-8}	

*At the center of the long straight section.

Fitting Table 5 shows the target parameters of the fitting and the knob settings. The lattice A has zero dispersion at the center of the long straight section, while in Lattice B the chromaticities have been corrected to zero by the sextupoles S2 and S3. Lattices A and B could be useful during the commissioning but not for the CSR operation. In Lattice C, we reduce α_1 to the nominal value of operation (1.9×10^{-3}) by introducing a dispersion of -0.17 m in the straights. However, the energy acceptance of Lattice C is less than 1% at the center of the straight section as shown by the RF bucket in Fig.4A. The higher order terms of α need to be reduced to enlarge the bucket height. This is done by using S1 and O3 (Lattice D) for the direct control of α_2 and α_3. With this fitting, α_4 becomes 1.09 and the RF bucket height increases to $\pm 3\%$ (Fig.4B). A particle tracking with this lattice also gives $\pm 3\%$ in straight and $\pm 2\%$ in the arc sections. Such momentum aperture distribution of

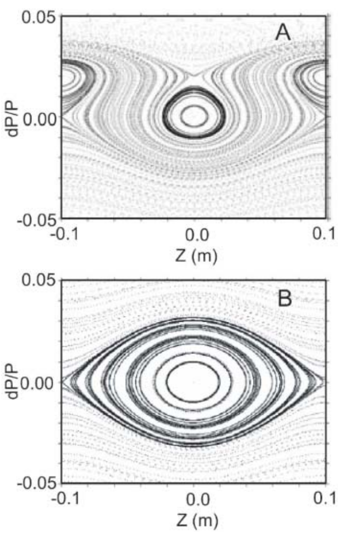

Figure 4: RF bucket for Lattices C and D

Lattice D gives a good Touschek beam lifetime as shown in Fig.5, where the calculations have been performed according to [4] with the assumption of a bunch length(σ_z) of 1 mm, energy spread of 5.0×10^{-4} and emittance of 7.0 $\times10^{-8}$ m·rad.

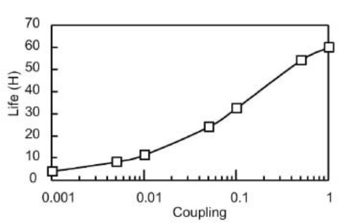

Figure 5: Touschek Lifetime

APPLYING THE FREQUENCY MAP ANALYSIS

Frequency map analysis[5][6] becomes fundamental in the design of CIRCE because of its strong non-linearities. The working point of ν_x=5.15 and ν_y=4.20 was chosen for the large dynamic aperture, by observing the behavior of its frequency map (Fig.6A) and dynamic aperture (Fig.6B). Here the frequency is calculated over 402 turns and the points in the map have frequency shift of less than 10^{-3}. The shift of the frequency distribution due to energy change is also considered on the map.

The extra knobs of O1 and Q2 can help to increase the dynamic aperture and we can see their effect on the frequency map. Figs.6C and D are for the case where O1=-65 m^{-3} and O2=70 m^{-3}. Note that the frequency distribution in the $\nu_x - \nu_y$ plane shrinks and the dynamic aperture increased.

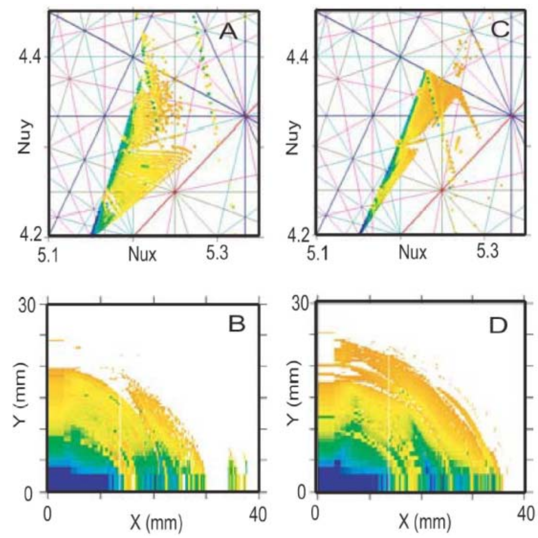

Figure 6: Frequency Map and Dynamic Aperture

CONCLUSION

We have developed a tool to design and analyze the CIRCE lattice and applied it for optimizing a lattice that fulfills to all the requirements on the momentum compaction and at the same time maintains a very good lifetime and dynamic aperture. The frequency map analysis was very helpful during the optimization process.

ACKNOWLEDGEMENT

We thank C. Steier for various discussion, especially on the frequency map analysis.

REFERENCES

[1] J. Byrd, et al. "CIRCE, the Coherent InfraRed CEnter at the ALS", EPAC 2004, July 2004.

[2] E. Forest and H. Nishimura,"Inclusion of Small Bending Radius and First Order Fringe Field Effects in the Calculation os the Natural Chromaticity and Dynamic Aperture of the ALS Storage Ring", LBNL ESG TECH NOTE-115, 1989.

[3] H. Nishimura, "Goemon, A C++ Library for Accelerator Modeling and Analysis", PAC 2001, Chicago, June 2001.

[4] Single and Multiple Touschek Effects, J. Le Duff, CERN Acc. School, 95-02,v2,P573

[5] J. Laskar, "Laskar, J. 1990 The chaotic motion of the solar system. A numerical estimate of the size of the chaotic zones", Icarus **88** 266-291, 1990.

[6] D. Robin, C.Steier, J. Laskar and L. Nadolski, "Global Dynamics of the Advanced Light Source Revealed through Experimental Frequency Map Analysis", PRL **85**, 558-561, 2000.